Applicability Analysis of Different Runoff Schemes of the Gulang River Basin in Arid Region of Gansu Province, China

Xiaojing Wang[1], *Lianguo* Zhao[1,*], *Jingnan* Zhang[1], *Tianyuan* Zou[1] and *Nan* Zhang[2]

[1]PIESAT International Information Technology Limited, Beijing, 100195, China
[2]Tianjin Normal University, Tianjin, 300387, China

Abstract. [**Background**] Mountain torrent disasters are one of the deadliest weather-related natural disasters in the world, often causing extremely serious economic and property losses and casualties; in recent years, due to heavy rainfall and complex geological and geomorphological conditions, mountain torrent disasters have occurred frequently in Gansu Province. An effective rainfall-runoff model is the key to prevent them. There are still many problems about how to establish suitable hydrological models in the arid basin of China. [**Methods**] Therefore, the Gulang River Basin in Gansu Province was selected as the research area to construct the HEC-HMS rainfall-runoff model; through the screening of different runoff methods, different runoff schemes were established to explore the optimal runoff algorithm for the arid basin; there are mainly SCS-CN method, initial and constant method, Green and Ampt method and exponential loss method in runoff generation; SCS unit hydrograph and Clark unit hydrograph methods are selected for slope transform, kinematic wave and lag algorithms for channel routing, totally 16 different runoff schemes. Three floods in the Gulang River Basin are selected to analyze the simulation effect of different runoff schemes in Gulang River Basin. [**Results**]1) If the Nash-Sutcliffe efficiency coefficient is selected as the evaluation index, the best simulation results are schemes 1 and 16 in the 20180826 flood, schemes 2 and 1 in the 20190626 flood and schemes 1 and 3 in the 20190911 flood. If the percentage of flood peak error is selected as the evaluation index, the best simulation results are schemes 16 and 1 in the 20180826 flood, schemes 9 and 6 in the 20190626 flood and schemes 13 and 4 in the 20190911 flood.If the percentage of runoff depth error is selected as indicator, the best simulation results are schemes 1 and 8 in the 20180826 flood, schemes 7 and 8 in the 20190626 flood and schemes 6 and 13 in the 20190911 flood. 2)The mean value of Nash-Sutcliffe efficiency coefficient obtained by the SCS-CN method for runoff generation, the SCS unit hydrograph for slope transform and the lag algorithm for channel routing are 0.8,0.65 and 0.65,respectively; the mean absolute percentage errors of flood peak are 9.29%,9.71% and 8.47%, respectively; the mean absolute percentage errors of runoff depth are 6.07%,7.17% and 7.74%, respectively; the mean time difference of flood peak of SCS unit hydrograph for slope transform and lag algorithm for channel routing are 1.21 hour and 1.5 hour, respectively.[**Conclusion**]The most suitable scheme is the combination of the SCS-CN method for runoff generation, SCS unit hydrograph for slope transform, and lag algorithm for channel routing. The results can provide a certain reference for the prevention of flood disasters in the arid region of Gansu Province.

1 Introduction

In recent years, due to heavy rainfall, and complex geological and geomorphic conditions, Gansu Province has experienced frequent flash flood disasters; among them, a flash flood disaster, occurred in Zhouqu County on August 7, 2010, causing 1,841 deaths and disappearances. On July 9-11, 2018, Gansu Province encountered the heaviest precipitation, among which the largest accumulated rainfall in Southeast Gansu reached 250 mm, inducing severe mountain torrent disasters and causing huge economy and property losses. In August 2020, Wenxian County suffered continuous heavy rains and severe waterlogging occurred in many county towns; Jingyuan County, suffered local torrential rains and severe mountain flood disasters occurred in some

townships. Obviously, effective flash flood disaster prevention technology is especially important for Gansu Province.

HEC-HMS is a semi-distributed hydrological model developed by the U.S. Army Engineers, which has been widely used to realize the simulation of rainfall-runoff processes through modular operation. For example, Wang Ruimin et al. constructed a hydrological model based on HEC-HMS for the Xingying River basin in southwest China, and performed parameter rate determination and model validation for multiple floods, and the results showed that the model simulated well. Tian Jing et al. developed a HEC-HMS model for the Guanshan River basin and analyzed the sensitivity parameters, and the results showed that the model simulated well. Ruting Liao et al. applied the HEC-HMS model to simulate multiple floods in Wenyu River basin,

---

*Corresponding author: ezhao_cn@163.com

and the results showed that the model simulation was well applicable. In China, the HEC-HMS model is commonly used for flood forecasting in watersheds, in which there are more studies on the application to wet areas and less studies on the application to arid areas. Therefore, in this paper, based on the HEC-HMS model, the Gulang River basin in Gansu Province is selected as the study area to explore the applicability of different production and confluence schemes in arid regions of China.

2 Study area and data

The Gulang River basin is located in the east end of the Hexi Corridor, in the middle of Gansu Province, between 102°42'~103°11'E and 37°9'~37°28'N. The terrain is high in the south and low in the north, with a temperate continental arid climate. Figure 1 shows the distribution of the water system and 25 rainfall observation stations in the Gulang River basin, with a basin area of 1,010 km2 and an elevation range between 2,080 and 4,298 m.

The DEM data of the study area were obtained from the geospatial data cloud platform, and analyzed by ArcGIS, to extract watershed characteristics, and the results are shown in Fig. 1. The land use types are mainly grassland, cropland and forested land (Fig. 2), and the soil types are mainly clay loam, sandy loam and loam (Fig. 3).
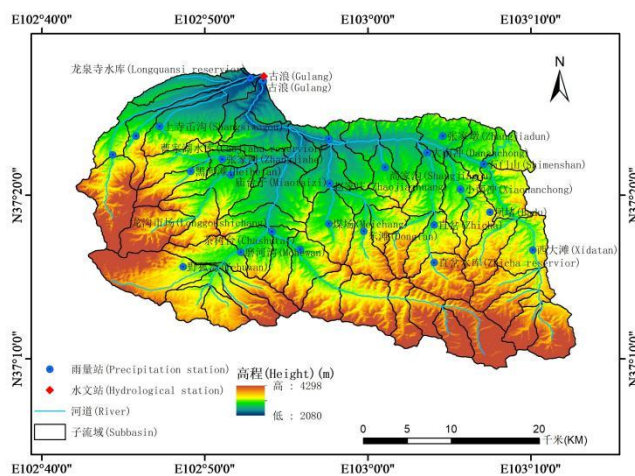

Fig. 1. Water system and station distribution map of Gulang River Basin
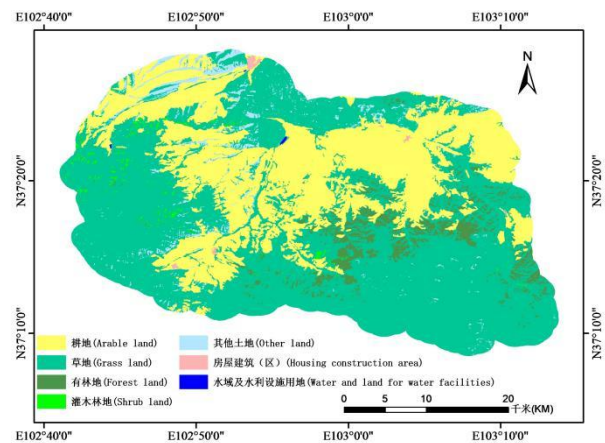

Fig. 2. Land use distribution map
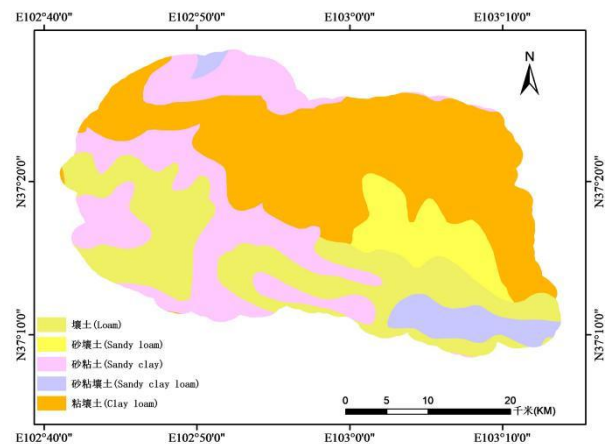

Fig. 3. Soil texture distribution map

3 Research Methodology

3.1 Production convergence program

The HEC-HMS model provides a variety of flow production and sink algorithms, so it can be combined into a variety of flow production and sink schemes by selecting different algorithms. In this paper, four flow-producing methods are selected, namely, exponential loss model, Green Amputation square model, initial loss followed by loss model and SCS-CN model; slope sink mainly selects Clark unit line and SCS unit line; river sink selects motion wave and hysteresis algorithm; base flow mainly adopts recession algorithm. According to the different methods selected for flow production, slope confluence and river confluence, a total of 16 sets of flow production and confluence schemes are established to analyze the applicability of different schemes in the Gulang watershed of Wuwei City, Gansu Province. For details, please see Table 1.

Table 1. Scheme table of the combination of different runoff methods

Schemes	Runoff generation	Slope transform	Channel routing	Base flow
Scheme 1	SCS-CN	SCS unit hydrograph	Lag algorithm	Recession
Scheme 2	SCS-CN	SCS unit hydrograph	Kinematic wave	Recession
Scheme 3	SCS-CN	Clark unit hydrograph	Kinematic wave	Recession
Scheme 4	SCS-CN	Clark unit hydrograph	Lag algorithm	Recession
Scheme 5	Initial and Constant	Clark unit hydrograph	Lag algorithm	Recession
Scheme 6	Initial and Constant	Clark unit hydrograph	Kinematic wave	Recession
Scheme 7	Initial and Constant	SCS unit hydrograph	Kinematic wave	Recession
Scheme 8	Initial and Constant	SCS unit hydrograph	Lag algorithm	Recession
Scheme 9	Green and Ampt	Clark unit hydrograph	Lag algorithm	Recession
Scheme 10	Green and Ampt	Clark unit hydrograph	Kinematic wave	Recession
Scheme 11	Green and Ampt	SCS unit hydrograph	Kinematic wave	Recession
Scheme 12	Green and Ampt	SCS unit hydrograph	Lag algorithm	Recession
Scheme 13	Exponential loss	Clark unit hydrograph	Lag algorithm	Recession
Scheme 14	Exponential loss	Clark unit hydrograph	Kinematic wave	Recession
Scheme 15	Exponential loss	SCS unit hydrograph	Kinematic wave	Recession
Scheme 16	Exponential loss	SCS unit hydrograph	Lag algorithm	Recession

In this paper, three floods occurred in the Gulang River basin, recorded as 20180823, 20190626, 20190911, with precipitation of 218 mm, 110 mm and 88 mm, and the basin outlet flood flows of 20.3 m3/s, 23.3 m3/s and 9.3 m3/s, with flood peaks of 3, 2 and 1, respectively; where rainfall data The Tyson polygon and weighting method were mainly used to calculate the average rainfall of sub-basins.

3.2 Error and accuracy evaluation

The simulation results are evaluated by three indexes, mainly the relative error of peak flow RQ, the Nash efficiency coefficient (N) and the peak-present time difference Δt; where the Nash efficiency coefficient reflects the degree of fit between the simulated runoff process and the actual measurement.

The evaluation indicators are calculated by the following formula.

$$R_Q = \frac{Q_s - Q_o}{Q_o} \times 100 \qquad (1)$$

$$N = 1 - \frac{\sum \left[Q_S(i) - Q_o(i) \right]^2}{\sum \left[Q_S(i) - Q_{o,mean} \right]^2} \qquad (2)$$

$$\Delta t = T - T^{'} \qquad (3)$$

Q_S, Q_o are the simulated and measured flow rate, m³/s; $Q_{o,mean}$ is the average of measured flow rate, m³/s; T, T'' are the measured flood occurrence time and simulated flood occurrence time, h. Where the closer R_Q approaches to 0 means the better of fitting effect,

the closer N approaches to 1 means the better of fitting effect, the closer Δt approaches to 0 means the simulated peak occurrence time domain is closer to the measured peak occurrence time.

4 Results and Analysis

Firstly, the initial values of the parameters of each scenario model are determined using the HEC-HMS model; then the measured flood data are used to rate and optimize the parameters of each scenario. According to Tables 2 and 3, it can be seen that if the larger Nash efficiency coefficient is selected as the evaluation index, the best results are scenario 1 and scenario 16 in the simulated flood of field 20180826; the best results are scenario 2 and scenario 1 in the simulated flood of field 20190626; the best results are scenario 1 and scenario 3 in the simulated flood of field 20190911. If the percent error of flood peak is selected as the evaluation index, the best results are scenario 16 and scenario 1 in the simulated flood of field 20180826; scenario 9 and scenario 6 in the simulated flood of field 20190626; and scenario 13 and scenario 4 in the simulated flood of field 20190911. If the percent error of runoff depth is selected as the evaluation index, the best results are scenario 13 and scenario 4 in the simulated 20180826 field floods, the best are scenario 1 and scenario 8; in the simulated 20190626 field floods, the best are scenario 7 and scenario 8; in the simulated 20190911 field floods, the best are scenario 6 and scenario 13.

According to the flood simulation results in Table 2 and Table 3, it can be seen that the average Nash efficiency coefficients for the three floods of SCS-CN, initial-loss-post-loss, Greenampot and exponential simulation for the flow production method selection are

0.8, 0.5, 0.56 and 0.68, respectively; the average absolute flood error percentages are 9.29%, 11.65%, 7.97% and 8.69%, respectively; the average absolute runoff depth error percentages 6.07%, 7.09%, 13.24% and 7.64%, respectively; therefore, the SCS-CN flow production method has the highest average Nash efficiency coefficient, while the average absolute flood error percentage flow production is the smallest using the Greene Amputation method and the average absolute runoff depth error percentage flow production is the smallest using the SCS-CN method.

The average Nash efficiency coefficients for the three floods were obtained for the slope confluence method by choosing SCS unit line and Clark unit line as 0.65 and 0.61; the average absolute flood peak error percentages were 9.71% and 9.09%; and the average absolute runoff depth error percentages were 7.17% and 9.85%, respectively. Therefore, the average Nash efficiency coefficients of the slope confluence method using SCS unit line and Clark unit line are not significantly different, while the average absolute flood peak error percentage is the smallest for Clark unit line and the average absolute runoff depth error percentage is the smallest for SCS unit line.

The average Nash efficiency coefficients of the river confluence methods selected are 0.62 and 0.65 for the kinematic wave and hysteresis algorithms, respectively; the average absolute flood peak error percentages are 10.33% and 8.47%, respectively; and the average absolute runoff depth error percentages are 9.28% and 7.74%, respectively. Therefore, the average Nash efficiency coefficients of the two methods of river confluence method kinematic wave and lagging algorithm are not very different, while the average absolute flood peak error percentage of lagging algorithm is the smallest and the average absolute runoff depth error percentage of lagging algorithm is the smallest.

By comparing the peak present time differences of the three floods simulated by different schemes, it can be seen that the average peak present time difference for the slope confluence using the SCS unit line method is 1.21 hours; the average peak present time difference obtained using the Clark unit line method is 1.18 hours; the average peak present time difference obtained using the river confluence using the motion wave method is 1.54 hours, and the average peak present time difference obtained using the lagging algorithm is 1.5 hours.

Table 2. Statistical table of flood simulation results for different floods

	Floods	Observation	Scheme 1	Scheme 2	Scheme 3	Scheme 4	Scheme 5	Scheme 6	Scheme 7	Scheme 8
Peak flow /(m³·s⁻¹)	20180826	20.30	20.60	21.50	18.80	18.10	19.50	21.80	23.10	22.60
	20190626	23.30	20.80	21.50	20.60	19.30	27.60	22.60	26.30	25.10
	20190911	9.30	10.20	10.60	8.50	8.70	10.70	11.70	10.50	10.00
Runoff depth /mm	20180826	53.35	53.74	53.98	46.61	46.43	47.99	50.68	53.77	53.65
	20190626	15.18	16.24	16.29	14.62	14.61	13.51	11.71	15.68	15.66
	20190911	13.98	14.67	14.73	13.06	13.04	13.77	13.79	12.20	12.19
Percentage of flood peak error/%	20180826		1.48	5.91	-7.39	-10.84	-3.94	7.39	13.79	11.33
	20190626		-10.73	-7.73	-11.59	-17.17	18.45	-3.00	12.88	7.73
	20190911		9.68	13.98	-8.60	-6.45	15.05	25.81	12.90	7.53
Percentage of runoff depth error/%	20180826		0.74	1.19	-12.62	-12.96	-10.04	-5.00	0.80	0.58
	20190626		6.93	7.27	-3.72	-3.77	-11.04	-22.87	3.27	3.16
	20190911		4.96	5.39	-6.55	-6.73	-1.47	-1.35	-12.73	-12.79
Time difference of flood peak /h	20180826		1	1	1	2	1	3	2	2
	20190626		1	0	2	2	1	2	2	2

	Floods								
	20190911	0	0	1	1	4	4	3	3
N	20180826	0.91	0.80	0.86	0.87	0.75	0.80	0.72	0.77
	20190626	0.87	0.93	0.64	0.54	0.72	0.58	0.35	0.32
	20190911	0.85	0.74	0.83	0.83	0.31	0.22	0.21	0.23

Table 3. Statistical table of flood simulation results for different floods

	Floods	Scheme 9	Scheme 10	Scheme 11	Scheme 12	Scheme 13	Scheme 14	Scheme 15	Scheme 16
Peak flow /(m³ · s⁻¹)	20180826	21.5	19.3	19.1	19.9	21.1	22	20.8	20.5
	20190626	23.8	24.6	24.2	26.5	25.3	25.3	29.3	25.9
	20190911	10.2	10.3	10.9	10.6	9.3	10.6	10.2	10.3
Runoff depth /mm	20180826	55.66	50.47	50.19	52.19	54.25	49.62	49.69	49.49
	20190626	11.15	11.22	11.64	13.89	13.11	13.17	13.75	13.69
	20190911	11.77	11.84	12.16	12.24	13.74	12.93	14.94	14.91
Percentage of flood peak error/%	20180826	5.91	-4.93	-5.91	-1.97	3.94	8.37	2.46	0.99
	20190626	2.15	5.58	3.86	13.73	8.58	8.58	25.75	11.16
	20190911	9.68	10.75	17.20	13.98	0.00	13.98	9.68	10.75
Percentage of runoff depth error/%	20180826	4.33	-5.39	-5.92	-2.16	1.70	-6.97	-6.85	-7.23
	20190626	-26.59	-26.08	-23.32	-8.51	-13.63	-13.29	-9.46	-9.86
	20190911	-15.79	-15.30	-13.04	-12.42	-1.71	-7.47	6.85	6.67
Time difference of flood peak /h	20180826	1	2	2	2	3	2	1	1
	20190626	1	1	1	1	2	2	1	1
	20190911	1	1	0	1	1	3	0	1
N	20180826	0.58	0.68	0.67	0.71	0.80	0.82	0.83	0.88
	20190626	0.73	0.73	0.76	0.72	0.52	0.51	0.75	0.73
	20190911	0.27	0.25	0.17	0.41	0.63	0.28	0.69	0.70

the flood simulation of field 20180826, for the first flood peak, the simulation results of scenarios 1-4 are better than those of scenarios 5-16, and also the overall simulation results of this flood are the best for scenarios 1-4. For the second flood peak of the 20190626 field flood, scenarios 5, 6 and 9-16 failed to simulate the second flood peak of this flood; while for the 20190911 field flood, the simulation results of scenarios 1-4 are better than those of scenarios 5-16. In conclusion, in the Gulang River basin of Gansu Province, the SCS-CN method is the best choice for the flow production method, followed by the exponential loss method, the SCS unit line is better than the Clark unit line for the slope

confluence, and the river confluence lag algorithm is better than the motion wave method.

5 Conclusion

In this paper, using the HEC-HMS model, 16 production and confluence flow schemes were established using different production and confluence methods to simulate three rainfall flood processes in the Gulang River basin. The results show that among the production flow methods, the SCS-CN method produces the best simulation results; among the slope confluence methods, the SCS unit line method produces better simulation

results than the Clark unit line method; among the river confluence methods, the hysteresis algorithm produces better simulation results than the motion wave method. Therefore, for the simulation of rainfall flood process in the Gulang River basin, it is suggested that the SCS-CN method is chosen for the flow production method, the SCS unit line is chosen for the slope confluence, and the lag algorithm is chosen for the river confluence. Since the object of this study is flooding in the hilly area in the arid region of northwest China, which usually has low vegetation cover and floods are usually sudden and short-lived, and the three hydrological processes of interception, depression filling and evaporation are neglected in this study when building the hydrological model, the subsequent study will further consider the three hydrological processes of interception, depression filling and evaporation.

Acknowledgements

References

1. B. Yong, W.C. Zhang, D.Z. Zhao et al. Application of hydrological modeling system HEC-HMS to Baohe catchment of Hanjiang Basin, Bulletin of Soil and Water Conservation, **2006(3)**, 86 (2006)

2. Z.Y. Liang, Y.W. Jia, K.J. Li, et al. Summary of application and study on distributional hydrologic model to flood forecasting, Yellow River, **29(2)**, 29 (2007)

3. R.M. Wang, H.X. Li, Q. Huang, et al. Flood forecasting of small-medium river in Southwest China using HEC-HMS model, Water Resources and Power, **39(1)**, 79 (2021)

4. J. Tian, J. Xia, Y.J. Zhang, et al. Application of HEC-HMS model in the Guanshan River Basin, Engineering Journal of Wuhan University, **54(1)**, 8 (2021)

5. R.T. Liao, S.S. Hu, L.G. Du, et al. Hydrological simulation of Wenyu River Basin based on HEC-HMS model[J].South-to-North Water Transfer and Water Science & Technology, **16(6)**,15 (2018)

6. Y. Li, X.T. Chen and C.X. Zhu, Application of HEC-HMS in flood forecasting, Yellow River, **30(4)**, 23 (2008)

7. Y.F. Kang, J.Z. Li and Q.S. Ma, Using HEC-HMS model to simulate flooding in Zijingguan watershed, Journal of Irrigation and Drainage, **38(4)**, 108 (2019)

8. L. Zhang, J. Li, X.R. Huang, et al. Application of HEC-HMS model for mountain flood forecasting in Qingxi River Basin, China Rural Water and Hydropower, **2020(1)**, 130 (2020)

9. Y. Zou, G.H. Hu, Z.X. Yu, et al. Application of HEC-HMS model for mountain flood forecasting in the Wushui Basin, Science of Soil and Water Conservation, **16(2)**, 95 (2018)

10. J.F. Li, W.C. Wang, P.P. Che, et al. Application research on HEC-HMS model and TOPMODEL model in mountain flood forecasting of Dongzhuang watershed, Water Resources and Power, **37(3)**, 50 (2019)

11. G.A. Tang, The experiment course of ArcGIS geographic information system spatial analysis, Beijing: The Science Publishing Company, (2006)

12. Z.G. Ma and L.L. Li, Hydrology information extracting of Yang River watershed based on GIS and DEM[J]. Journal of Hebei North University (Natural Science Edition), **24(1)**, 69 (2008)

13. G.M. Qin and R. Dai, Acquisition of basin characteristics based on GIS and DEM-A case study of Jitaiqu watershed, Northwest Hydropower, 2010 (13):4 (2010)

14. R. Dai and Z.F. Wang Application of GIS Technology in Calculation of Design Runoff of Basins, Northwest Hydropower, **2012(3)**, 1 (2012)

15. L.M. Zhang, W.H. Liao, Z.K. Yin, et al. Application of the HEC-HMS model for calculating the local inflow of giant reservoir group in Xijiang River Basin, China Rural Water and Hydropower, **2017(6)**, 65, (2017)

16. M. Saidi, A. Shalamu, J.L. Ding, et al. Application of HEC-HMS in data-insufficient mountainous watersheds-A case study from Urumqi River Basin, Bulletin of Soil and Water Conservation, **35(6)**, 140 (2015)

17. J.T. Wang, Simulation and research of mountain flood early warning in typical small watershed in North China based on HEC-HMS model, University of Jinan, (2018)

18. A.D. Feldman, Hydrologic Modeling System HEC-HMS, Technical Reference Manual. Technical Reference Manual, (2000)